

# Cholesterol gallstone dissolution in bile: dissolution kinetics of crystalline (anhydrate and monohydrate) cholesterol with chenodeoxycholate, ursodeoxycholate, and their glycine and taurine conjugates

Hirotsune Igimi and Martin C. Carey<sup>1</sup>

Department of Medicine, Harvard Medical School, Division of Gastroenterology, Peter Bent Brigham Hospital (Brigham and Women's Hospital, Inc.) and Harvard University–Massachusetts Institute of Technology, Division of Health Sciences and Technology, Boston, MA 02115

**Abstract** The dissolution kinetics of the common crystalline forms of cholesterol (anhydrate and monohydrate) were studied in free and conjugated chenodeoxycholate and ursodeoxycholate solutions by static disk, rotating disk, and powder dissolution techniques. The dissolution kinetics of both forms of cholesterol were found to be non-diffusion controlled, i.e., the detachment rate of cholesterol molecules from the solid crystals was rate-limiting. Cholesterol dissolution rates in chenodeoxycholate solutions were significantly faster than in ursodeoxycholate solutions, and micellar solubilities and dissolution rates of anhydrous cholesterol were appreciably larger than those of cholesterol monohydrate. In free and conjugated chenodeoxycholate solutions, the higher solubilities of anhydrous cholesterol converged to the lower solubilities of the monohydrate within a few days, but in ursodeoxycholate solutions “anhydrous” cholesterol remained metastable for weeks. Cholesterol dissolution rates were accelerated in proportion to increases in the bile salt and neutral electrolyte (NaCl) concentration and correlated closely with the cholesterol solubilizing capacity of the bile salts (free bile salts  $\gg$  glycine conjugates  $>$  taurine conjugates). Dissolution rates were also increased by increases in temperature (17–47°C), but no change was observed at the polymorphic crystalline transition temperature of anhydrous cholesterol (39°C). Linear extrapolations of the temperature dependence of the dissolution rate constants for both forms of cholesterol converged at higher temperatures and intersected at 86.7°C. This temperature has been shown by other methods to be the transition temperature where cholesterol monohydrate is converted to the anhydrous form. Dissolution rates were retarded markedly by partial protonation of the bile salt suggesting that sparingly soluble bile acids and cholesterol may compete for micellar binding sites. These studies suggest that micellar dissolution rates of cholesterol gallstones during therapy with ursodeoxycholic acid should be appreciably slower than during therapy with chenodeoxycholic acid. Since the clinical efficacy of gallstone dissolution with either agent appears to be similar, it is concluded that physical-chemical mechanisms other than

micellar solubilization may be operative in ursodeoxycholate-induced gallstone dissolution.—**Igimi, H., and M. C. Carey.** Cholesterol gallstone dissolution in bile: dissolution kinetics of crystalline (anhydrate and monohydrate) cholesterol with chenodeoxycholate, ursodeoxycholate, and their glycine and taurine conjugates. *J. Lipid Res.* 1981. **22:** 254–270.

**Supplementary key words** static disk apparatus · rotating disk apparatus · powder dissolution · equilibrium solubility · dissolution rate · dissolution rate constant · diffusion controlled dissolution · non-diffusion controlled dissolution · Noyes-Nernst equation · Levich equation

Cholesterol, which is universally distributed in animal tissues, is both a vital and lethal sterol. It plays a key structural and functional role in cell membranes, serum lipoproteins, and in the mixed micelles of bile. Two strategic tubular organ systems bear the brunt of excess cholesterol deposition: cholesterol monohydrate constitutes the major component of most gallstones (1, 2) and cholesterol monohydrate together with cholesteryl esters composes the lipid lesion of atherosclerosis (3). Less commonly, cholesteryl esters may form liquid crystalline accumulations in the liver, gallbladder wall, and reticulo-endothelial systems (4).

Abbreviations: CDC, chenodeoxycholate; UDC, ursodeoxycholate; C, cholate; DC, deoxycholate; T-, G-, prefixes indicate taurine and glycine conjugates, respectively; ChA, anhydrous cholesterol (polymorphic form not specified); ChM, cholesterol monohydrate; GLC, gas-liquid chromatography; TLC, thin-layer chromatography; HPLC, high performance liquid chromatography.

<sup>1</sup> Address correspondence and reprint requests to this author at the Peter Bent Brigham Hospital (Division of Brigham and Women's Hospital, Inc.), 75 Francis Street, Boston, MA 02115.

Whereas reversal of deposited cholesterol in the arterial intima is not yet a practical therapeutic measure, considerable success has been achieved in recent years in dissolving cholesterol gallstones in the gallbladder and bile ducts by medical means. The ingestion of two specific bile acids, chenodeoxycholic ( $3\alpha,7\alpha$ -dihydroxy- $5\beta$ -cholanoic, CDC) acid or its  $7\beta$ -hydroxy epimer, ursodeoxycholic ( $3\alpha,7\beta$ -dihydroxy- $5\beta$ -cholanoic, UDC) acid, decreases cholesterol secretion into bile (5), desaturates bile with cholesterol (5), and induces slow dissolution of gallstones in about a quarter to a third of patients (6).

Since a detailed understanding of the dissolution kinetics of cholesterol from biological precipitates is of considerable theoretical as well as therapeutic importance, the aims of the present study are: *i*) to identify quantitatively the kinetic factors which control the dissolution rates of gallstones with both CDC and UDC, especially since these bile acids differ markedly in their cholesterol solubilizing capacities (7), *ii*) to compare the dissolution kinetics of cholesterol monohydrate (ChM) with anhydrous cholesterol (ChA) (8) (even though the latter is not found in gallstones, it may well be the chemical form of cholesterol in biological membranes and in the interior of other macromolecular lipid aggregates),<sup>2</sup> and *iii*) to identify and evaluate possible physical-chemical factors which might accelerate or retard gallstone dissolution *in vivo*.

We establish that dissolution rates and maximum micellar solubilities of ChA are significantly greater than ChM irrespective of the bile salt species. ChA and ChM dissolution is much faster in solutions of CDC and its conjugates than in solutions of UDC and its conjugates, and in each case the dissolution kinetics are non-diffusion controlled. Thus the 'stone'-solution interfacial reaction is rate-limiting for gallstone dissolution by bile salts and this reaction is slower for ChM than for ChA. These data suggest that with our present inability to shake the gallbladder mechanically *in situ* the prospects for accelerating gallstone dissolution by chemical means are not good.

## EXPERIMENTAL PROCEDURE

### Materials

Cholesterol (Nu-Chek Prep, Austin, MN) was recrystallized thrice from hot 95% EtOH and mixed with [1, 2-<sup>3</sup>H]cholesterol (New England Nuclear Co., Boston, MA) to provide, as required,  $\approx 5$  gram batches

<sup>2</sup> Mazer, N. A., G. B. Benedek, and M. C. Carey. Submitted for publication.

of specific activity of 1 mCi (CDC studies) or 5 mCi (UDC studies) per 5 g. After short-term storage at  $-20^{\circ}\text{C}$  under  $\text{N}_2$ , the samples were chemically and radiochemically pure by gas-liquid chromatography (GLC) and thin-layer chromatography (TLC) with zonal scanning. Crystalline unconjugated CDC and UDC acids of  $\approx 99\%$  purity (TLC, GLC) were generously supplied by Dr. Herbert Falk (Dr. Falk GmbH & Co., Freiburg, West Germany) and were converted to the sodium salts as described (9). The glycine (G) conjugates of similar purity were generously custom-synthesized by the Tokyo Tanabe Pharmaceutical Co. (Tokyo, Japan) and were supplied as sodium salts. The taurine (T) conjugates were purchased from Calbiochem (San Diego, CA) and were generally about 98% pure by TLC and high performance liquid chromatography (HPLC) employing an octadecylsilane reversed phase column. One-percent solutions of both T conjugates were potentiometrically titrated with 2 N HCl and when a correct titration curve was not obtained the sample was recrystallized prior to study (9, 10). Samples of other common bile salts, cholate (C), deoxycholate (DC), and their T and G conjugates (Calbiochem, San Diego, CA) were of similar purity (TLC, HPLC) after recrystallization (9). Benzoic acid was obtained from Fisher Scientific (Boston, MA) and was  $\approx 99.8\%$  pure by elemental analysis. All other chemicals were A.C.S. and/or reagent grade. Roasted NaCl ( $600^{\circ}\text{C}$ ), carbonate-bicarbonate or phosphate buffers, ion-exchanged, filtered and glass-distilled water, and acid-alkali-washed Pyrex-brand glassware were used throughout (9, 10).

### Methods

*Anhydrous cholesterol (ChA).* Five g of recrystallized [1, 2-<sup>3</sup>H]cholesterol was dissolved in hot ( $70^{\circ}\text{C}$ ) MeOH (350 ml) and the solution was cooled *quickly* to  $4^{\circ}\text{C}$ . The precipitated crystals were filtered through a 10–15 mesh autoclaved fritted glass filter in a Buchner Funnel (Fisher Scientific, Boston, MA) and the MeOH was evaporated overnight *in vacuo* at  $80^{\circ}\text{C}$ . The dry crystals were then stored in a darkened desiccator for short periods of time over  $\text{CaSO}_4$ .

*Cholesterol monohydrate (ChM).* Five g of recrystallized [1, 2-<sup>3</sup>H]cholesterol was dissolved in 95% EtOH (400 ml) at  $60^{\circ}\text{C}$ . The solution was *slowly* cooled to room temperature ( $\approx 23^{\circ}\text{C}$ ) and then seeded with a few crystals of pure ChM (11). By 48 hours, a generous crop of ChM crystals had precipitated from the mother liquor and these were harvested by filtration as described above and then dried overnight in a desiccator thermostatted at  $40^{\circ}\text{C}$ . The crystals were stored for brief periods at  $23^{\circ}\text{C}$  in a darkened des-

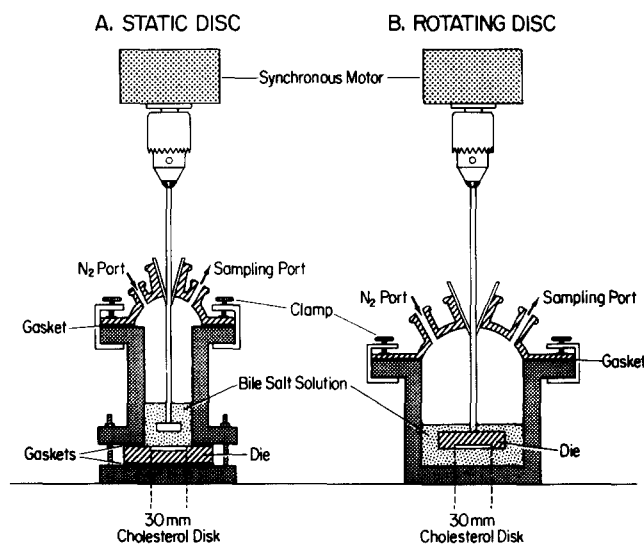


**Fig. 1.** Diagrammatic representation of A, static disk and B, rotating disk apparatus for dissolution rate and equilibrium solubility studies. Only small volumes of bile salt solutions are required (25 ml in A and 50 ml in B).

sicator in an  $N_2$  atmosphere that was saturated with water vapor.

Capillary melting points, direct and polarized light microscopy, and X-ray powder diffraction patterns (courtesy of Dr. Marc Grympas, Children's Hospital Medical Center, Boston, MA) verified that the cholesterol crystals obtained were pure and identical to authentic ChA and ChM, respectively (8). Thermogravimetric analysis of ChM after low temperature drying indicated that  $1.0 \pm 0.2$  molecules of  $H_2O$  were bound to each cholesterol molecule. Similar analysis of ChA produced no change in weight and confirmed that the crystals were anhydrous.

## EXPERIMENTAL DESIGN

### Dissolution apparatus (12)

**Static disk method.** For most dissolution experiments, thin (0.75–1.55 mm) disks of ChA or ChM were prepared by compressing a weighed amount of cholesterol crystals in an evacuated stainless steel die, 30.0 mm (i.d.) under a pressure of 10,000 p.s.i., (Carver Laboratory Press, Fisher Scientific, Boston, MA). The die containing the cholesterol disk was then sealed between two Teflon gaskets to become the bottom of a stainless steel cylinder (**Fig. 1A**). A glass cap with three ports was clamped over the top of the cylinder and an impeller rod of a synchronous variable speed motor was inserted through a Teflon collar in the central opening. The rod terminated in a stirring paddle which was held vertically 10 mm above the

cholesterol disk. The two other ports were sealed with Teflon bungs and were opened periodically for flushing with  $N_2$  and sampling. After addition of a bile salt solution, the glass top was hermetically sealed with four screw clamps to the dissolution chamber (**Fig. 1A**). Then the stainless steel part of the assembly was immersed in a constant-temperature water bath for the duration of the experiment.

**Rotating disk method.** This configuration and the accompanying Levich theory (see equation below) was employed to examine the relative contributions of diffusion and interfacial kinetics to the control of cholesterol dissolution. As in the static disk apparatus, thin cholesterol disks (0.75–1.5 mm) were prepared in a stainless steel die of 30.0 mm (i.d.) under a pressure of 10,000 p.s.i. The inverted die plus cholesterol disk was then screwed onto the tip of a straight stainless steel impeller rod, the free end of which exited through Teflon collars in the central opening of the glass cap to become the drive shaft of a synchronous motor (**Fig. 1B**). Thus the die-tipped impeller rod held the cholesterol disk upside down within the sealed dissolution chamber ensuring that the cholesterol surface was exactly 10 mm above the bottom. After the addition of a bile salt solution, the motor was switched on to rotate the cholesterol disk at constant r.p.m. (40–800). Sampling, gassing with  $N_2$ , and temperature control during the period of dissolution were carried out exactly as described for the static disk system.

**Powder dissolution method (10).** To determine equilibrium micellar solubilities and to ensure rapid hydration of ChA  $\rightarrow$  ChM and nucleation, cholesterol crystals were first finely powdered in an agate mortar and an excess ( $\approx 500$  mg) was introduced into 10 ml of the bile salt solution in a small dissolution chamber (not shown). The dissolution vessel was sealed under  $N_2$ , immersed in a water bath at  $37^\circ C$ , and shaken continuously for several weeks. At suitable time intervals, samples were withdrawn through a sampling port, filtered through  $0.22 \mu m$  Millipore filters to separate the micellar phase from excess cholesterol, and the mixed micellar filtrates were assayed in triplicate for cholesterol as described below.

**Bile salt solutions.** Bile salt solutions were composed on a weight/volume basis in carbonate-bicarbonate buffers at pH 10.0 (free bile salts and glycine conjugates) or pH 7.0 (taurine conjugates) or in phosphate buffers when variation in pH was required. The other conditions were 0.15 M  $Na^+$ , 100 mM bile salt concentrations at  $37^\circ C$ , but these were varied for specific experimental purposes as described below. The initial working volumes of the bile salt solutions were 25 ml (static disk experiments) or 50 ml (rotating

disk experiments) and small (50–200  $\mu\text{l}$ ) samples were taken at suitable intervals for cholesterol analysis. During each experiment the stirring speed was maintained constant (usually 300 r.p.m.) and since neither the surface area of the cholesterol disks nor the solution volume changed appreciably during the course of an experiment, the only measured variable was the dissolution rate of cholesterol.

**Chemical analyses.** Micellar cholesterol concentrations were determined from measurements of radioactivity in the samples using a liquid scintillation spectrometer. In experiments where dissolution to equilibrium was carried out, the final solubility of cholesterol was also checked with both the cholesterol oxidase and Leibermann-Burchard methods (13, 14) and was found to be identical. The concentration of benzoic acid dissolved during dissolution in water (pH 7.0) was assayed spectrophotometrically at 270 nm.

### Dissolution theory

Our general theoretical model for dissolution of crystalline cholesterol in bile salt micellar solutions implies three steps: *i*) a cholesterol-unsaturated bile salt micelle in the bulk solution diffuses through a diffusion (“unstirred”) layer to the cholesterol disk-solution interface, *ii*) the micelle incorporates a cholesterol molecule(s) from the crystalline solid, and then *iii*) diffuses away returning to the bulk solution.

**Diffusion controlled dissolution** (15, 16). This theory assumes that the surface incorporation of cholesterol molecules is extremely fast compared with diffusion. Hence in the steady state, the micelles are saturated in the aqueous layer next to the surface (the “saturated layer”) (Fig. 2A). Once the surface of the cholesterol disk is covered by the “saturated layer,” further dissolution of cholesterol molecules will not occur. Noyes and Whitney (15) and Nernst (16) determined that the rate at which a solid substance dissolved in its own solution is proportional to the difference between the concentration of that solution ( $C$ ) and the concentration of the saturated solution ( $C_s$ ), i.e.,

$$\frac{dC}{dt} = K(C_s - C) \quad \text{Eq. 1a}$$

where  $dC/dt$  gives the dissolution rate<sup>3</sup> and  $K$  is the proportionality constant or the apparent dissolution rate constant. However, since  $K$  is proportional to the

<sup>3</sup> In this paper we will follow common practice and call  $dC/dt$  the dissolution rate. However, the reader should bear in mind that it is more correct to use  $V(dC/dt)$  (Fig. 1b) as the dissolution rate.  $dC/dt$  is the change in the concentration of solute occurring in the solvent per unit time, whereas  $V(dC/dt)$  is the amount of solute dissolved per unit time.

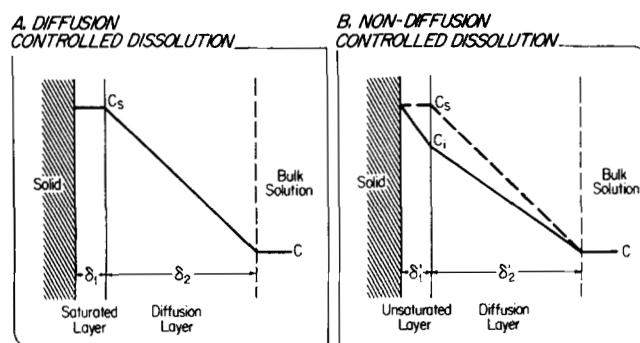


**Fig. 2.** Schematic diagrams of theoretical solution concentration profiles during the dissolution of crystalline cholesterol disks. A: Diffusion-controlled dissolution; B: non-diffusion-controlled dissolution.  $C$ : concentration of cholesterol in bulk solution;  $C_s$ , saturated concentration of cholesterol in the “saturated layer” at disk-solution interface;  $C_i$ , effective concentration of cholesterol at disk-solution interface;  $\delta_1$  and  $\delta'_1$ , thickness of “saturated” and “unsaturated” layers in A and B, respectively;  $\delta_2$  and  $\delta'_2$ , thickness of diffusion layers.

surface area of the cholesterol disk ( $S$ ) and inversely proportional to the volume of solution ( $V$ ), we can rewrite equation (1a) as

$$\frac{dC}{dt} = \frac{S}{V} k(C_s - C) \quad \text{Eq. 1b}$$

where  $k$  is now the dissolution rate constant.

Levich (17) established that the rate constant  $k$  (Eq. 1b) for a diffusion controlled process (in his case adsorption to a disk rotating in a fluid at rest) was

$$k = 0.625 D^{2/3} \times \nu^{-1/6} \times \omega^{1/2} \quad \text{Eq. 2}$$

where  $D$  ( $\text{cm}^2 \cdot \text{sec}^{-1}$ ) is the diffusion coefficient (i.e., of micelles),  $\nu$  is the kinematic viscosity of the solution ( $\text{cm}^2 \cdot \text{sec}^{-1}$ ) and  $\omega$  is the angular velocity of rotation in radians  $\text{sec}^{-1}$  ( $2\pi \times \text{r.p.s.}$ ) at the disk-solution interface. Hence for a diffusion-controlled process, a plot of  $k$  (obtained from Eq. 1b) versus  $\omega^{1/2}$  in a rotating disk experiment should be linear with a zero intercept, since we can assume that  $D$  and  $\nu$  are both constant over a moderate range of rotating rates where bulk fluid rotation and turbulence are avoided (Eq. 2).

**Non-diffusion controlled dissolution** (18, 19). In contrast to diffusion-controlled dissolution, the rate of incorporation of cholesterol molecules from surface to solution in this case is slow compared with the diffusion steps. The extreme case is where the incorporation rate is infinitely slow and dissolution becomes interfacially-controlled. In actual practice, the dissolution rates of most solutes involve both components (interfacial reaction rate and diffusion rate) which we will term here “non-diffusion controlled dissolution.” In Fig. 2B we show a concentration profile for a solute dissolving from a solid

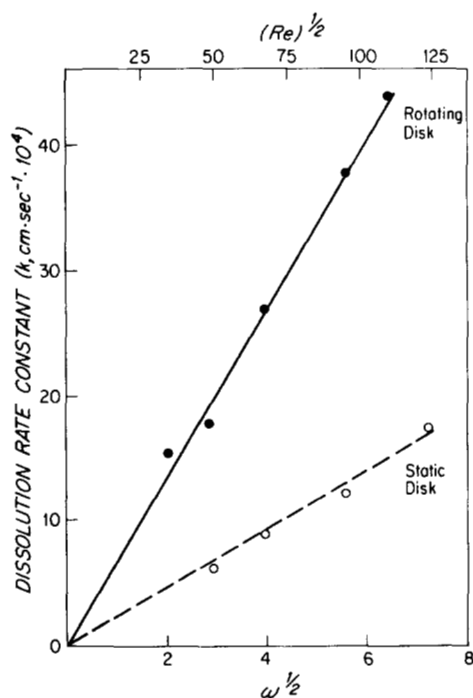


Fig. 3. Dissolution rate constants ( $k$ ) of solid benzoic acid dissolving in water plotted as a function of the square root of the angular velocity ( $\omega^{1/2}$ ) and Reynold's Number ( $Re^{1/2}$ ).

surface into solution under these conditions. This is superficially similar to that in Fig. 2A (diffusion-controlled dissolution), but now  $\delta'_1$  indicates that a concentration gradient exists where a "saturated layer" was present in the earlier configuration. By comparing the solid lines in Figs. 2A and 2B we see that  $C_i$  is less than  $C_s$  and  $\delta'_2$  is the diffusion layer as before. By analogy with the Noyes-Nerst treatment we can describe the dissolution rates as being dependent on two consecutive first order reactions (20), the surface reaction followed by the diffusion step. In this case, instead of equation 1b, we obtain equations 3a and 3b.

$$\frac{dC}{dt} = \frac{S}{V} \frac{krkt}{kr + kt} (C_s - C) \quad \text{Eq. 3a}$$

$$= \frac{S}{V} \kappa (C_s - C) \quad \text{Eq. 3b}$$

This equation is analogous to equation 1a, but now the effective rate constant  $\kappa$  is

$$\kappa = \frac{krkt}{kr + kt} \quad \text{Eq. 3c}$$

where  $kr$  and  $kt$  are the first-order rate constants for the interfacial reaction and the diffusion step, respectively. This is simply an expression for two conductances in series.

Since  $k$  in Eq. 2 is  $kt$  in Eq. 3a, we can combine Levich's equation (Eq. 2) with Eq. 3a:

$$\frac{1}{\kappa} = 1.612D^{-1/3} \times \nu^{1/6} \times \omega^{-1/2} + \frac{1}{kr} \quad \text{Eq. 4a}$$

$$= A\omega^{-1/2} + B \quad \text{Eq. 4b}$$

Then if we plot  $1/\kappa$  (from experiment) versus  $\omega^{-1/2}$ , the positive intercept ( $B$ , Eq. 4b) will give the reciprocal of the interfacial rate constant ( $1/kr$ ), i.e., the interfacial resistance. Therefore, both equations 3b and 4a allow us to estimate independently the relative contributions of interfacial and diffusional factors involved in cholesterol dissolution. A linear slope in plots of this equation ( $A$ , Eq. 4b) confirms that  $D$  and  $\nu$  are constant between specific rotating speeds.

## RESULTS

### Influence of cholesterol disk-pressure on dissolution rates

In preliminary experiments, ChM disks were made with pressures which varied from 2000 to 10,000 p.s.i. in 2000 p.s.i. increments. Their dissolution rates were studied by the static disk method in 100 mM CDC at 37°C (stirring rate 300 r.p.m.). The dissolution rates were fastest with the 2000 p.s.i. disks ( $k \times 10^4 = 2.57 \text{ cm} \cdot \text{sec}^{-1}$ ) and decreased in direct proportion to increases in disk-pressure, only becoming constant when the compressions reached 8000 p.s.i. ( $k \times 10^4 = 2.03 \text{ cm} \cdot \text{sec}^{-1}$ ). To eliminate the effects of this potential variable on our results, we employed disk compressions of 10,000 p.s.i. for all subsequent dissolution experiments.

### Influence of rotating speed on the dissolution rates of benzoic acid in water

In order to validate the apparatus and the theories employed to analyze our results quantitatively, we determined the dissolution rates and dissolution rate constants for solid benzoic acid in water, a compound whose dissolution kinetics is known to be close to diffusion controlled (21–23). In Fig. 3, we plot the dissolution rate constant ( $k$ ) versus the square root of  $\omega$ , the angular velocity<sup>4</sup> from experimental data em-

<sup>4</sup> The square root of Reynold's number ( $Re^{1/2}$ ) which corresponds to the square root of the angular velocity,  $\omega^{1/2}$  is also plotted on the abscissa of the graphs where a rotating disk geometry was employed.  $Re = r^2\omega\rho/\mu$ , a dimensionless number, where  $\omega$  is the angular velocity ( $2\pi \times \text{r.p.s.}$ ),  $r$  is the disk's radius (1.50 cm),  $\rho$  is the density of the solution (g/ml) which for a 100 mM CDC solution is 1.28 and  $\mu$  is the solution viscosity taken as  $0.01 \text{ g} \cdot \text{cm}^{-1} \cdot \text{sec}^{-1}$ .  $Re^{1/2}$  and  $\omega^{1/2}$  can only be equated in a rotating disk experiment since the angular velocity at the disk-solution interface is known with certainty only when the disk (and not the solution) is rotated at a constant rate.

employing the rotating disk and static disk methods. As predicted by Levich's equation (Eq. 2), the rotating disk data is linear and passes through the origin. As indicated in footnote 4, these results are valid only for the rotating disk experiments. Even though the static disk data also intersects the origin, the  $k$  values at any value of  $\omega^{1/2}$  are significantly less than the rotating disk results. Thus at zero stirring rates, if the conditions were truly stagnant, no dissolution of benzoic acid should be possible.<sup>5</sup>

#### Influence of stirring speed on dissolution rates of ChM in CDC solutions—static disk method

In order to determine a suitable stirring speed for subsequent experiments, the dissolution rates of ChM were determined in 100 mM CDC (37°C, pH 10.0) for stirring rates which varied between 40–500 r.p.m. (Fig. 4). The dissolution rates increase progressively with increasing stirring rates to 300 r.p.m. and then fall slightly at 500 r.p.m. The inset shows the increase in dissolution rate constant ( $k$ ) as a function of increases in stirring speed ( $\omega^{1/2}$ ). Even though the Levich equation cannot be applied to static disk dissolution studies owing to the complexity of the velocity profile at the surface of the disk, the data suggest (as is proven subsequently) that ChM dissolution is not diffusion-controlled in view of the large positive intercept at zero stirring rates. A stirring rate of 300 r.p.m. was used routinely for most of the subsequent dissolution experiments.

#### Dissolution of ChM and ChA in solutions of CDC and UDC and their conjugates—static disk method

The dissolution rates of ChM in 100-mM solutions of CDC and its conjugates and in UDC and its conjugates are displayed in Fig. 5A and the dissolution rates of ChA in 100-mM solutions of CDC, GCDC, TCDC, and UDC are plotted in Fig. 5B, respectively. As the amount of cholesterol dissolved increases as a function of time, the dissolution rates decrease and level off as micellar saturation is approached. In each case initial dissolution rates and final solubilities of ChA are appreciably greater than ChM, with the former displaying no evidence of nucleation over the duration of the experimental period (20 hr). The dissolution rates and solubilities of both ChM and ChA are markedly (up to 20-fold) greater in CDC solutions than in UDC solutions. The equilibrium solubilities,

<sup>5</sup> In real systems even when there is no stirring, conditions are usually not stagnant because of natural convection from pressure, temperature and density fluctuations in the solvent. Hence some dissolution of diffusion controlled substances always occurs in the absence of stirring.

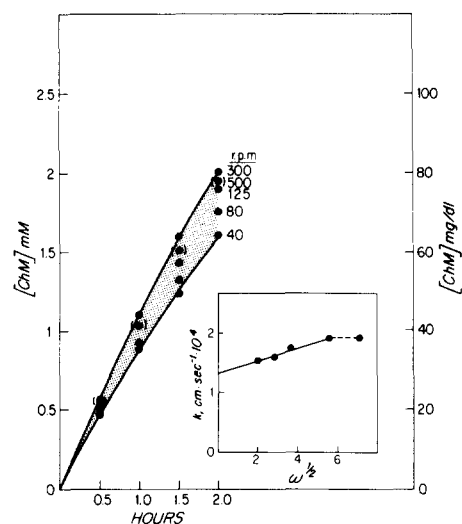


Fig. 4. Influence of stirring speed (r.p.m.) on the dissolution rates of static disks of cholesterol monohydrate (ChM) (100 mM CDC, 37°C, pH 10.0, 0.15 M Na<sup>+</sup>, 25 ml). Inset: dissolution rate constants ( $k$ ) versus the square root of the impeller's angular velocity ( $\omega^{1/2}$ ) in radians·sec<sup>-1</sup>.

saturation ratios, dissolution rates, and dissolution rate constants calculated from the curves in Fig. 5A and B are listed in Table 1. These data show that the magnitude of the dissolution rates have the rank order of ChA > ChM, free bile salts > conjugates, and CDC series  $\gg$  UDC series. Further, the dissolution rate constants ( $k$ ) for the CDC series are about 2 to 3-fold larger than the rate constants for the UDC series.

#### Powder dissolution studies of ChM and ChA in solutions of CDC, UDC, and their conjugates

Since the maximum ChA solubility in each bile salt solution was higher than that of ChM (Table 1, Fig. 5A and B) and was stable for the duration of the static disk experiments (20 hr), we carried out dissolution experiments using an excess of finely powdered cholesterol (ChA and ChM) (see Methods) in order to induce nucleation of the bile salt systems which had become supersaturated with ChM (Fig. 6A, 6B). In the case of CDC and its conjugates, an initial peak in cholesterol solubility is reached during the first day of dissolution and thereafter these higher solubilities approach the equilibrium ChM values. After 2–4 days, both ChM and 'ChA' solubilities become identical (Fig. 6A, 6B) and remain so for the duration of the experiment. In the case of UDC (Fig. 6A and 6B), the higher solubilities of ChA took 3–4 days to attain the lower solubility of ChM but in the case of GUDC and TUDC, no nucleation of hydrated ChA was evident over the 21-day experimental period (Fig. 6B).

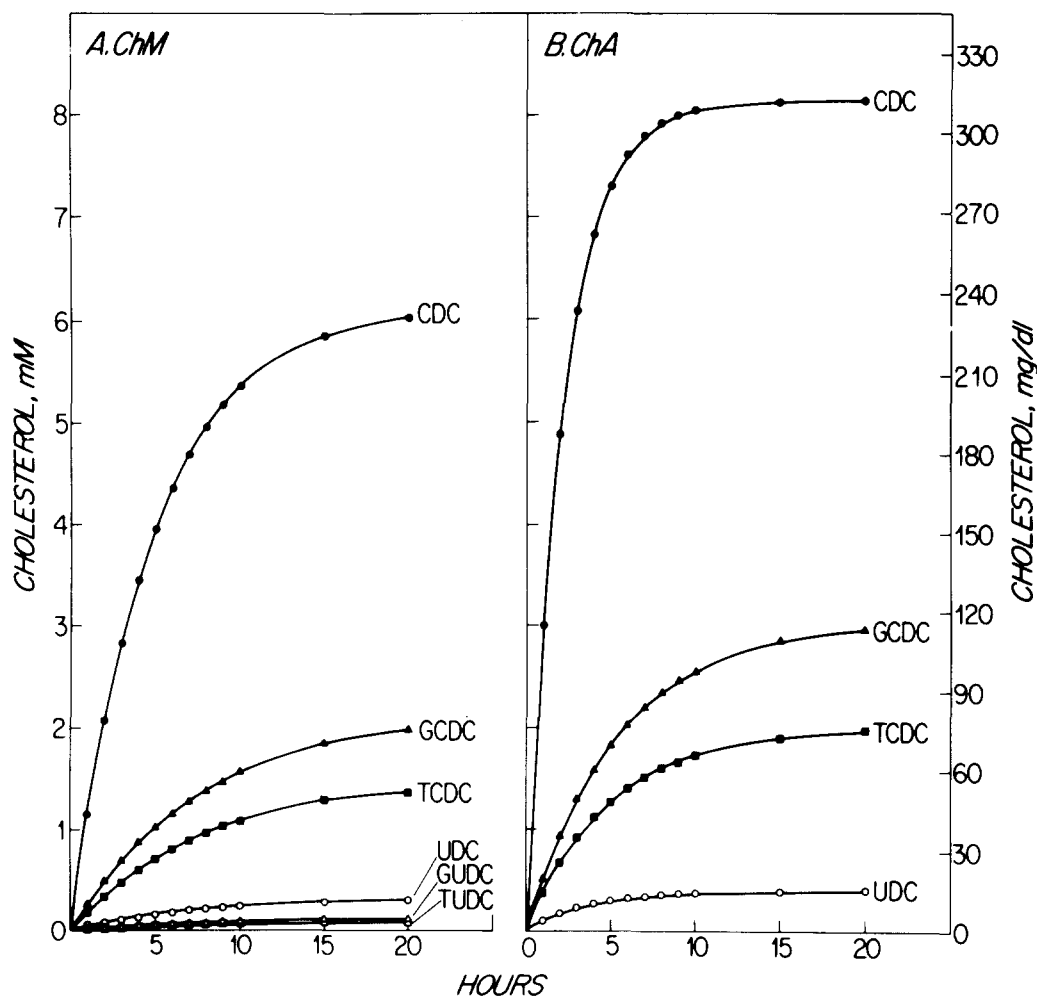


Fig. 5. Dissolution rates of A: cholesterol monohydrate (ChM) and B: anhydrous cholesterol (ChA) in 100 mM bile salt solutions by the static disk method (300 r.p.m., 37°C, 0.15 M Na<sup>+</sup>, pH 7.0 (taurine conjugates) and pH 10.0 (free and glycine conjugates). See list for bile salt abbreviations.

#### Influence of pH and ionic strength on ChM dissolution rates in CDC solutions—static disk method

Because both CDC, UDC, and GUDC can precipitate from aqueous systems at pH values which fall within the physiological range (9), we determined the initial dissolution rates of ChM in 100 mM CDC (37°C) at pH values of 10.0, 9.2, 8.1, and 7.4 (Fig. 7A). The dissolution rate decreases appreciably once protonation of the bile acid commences (pH = 9.0) and at pH 8.1 and 7.4, when mixed micelles of ionized CDC and its acid form are present, the dissolution rates are reduced compared to pH 10.0. Increases in ionic strength (NaCl) from 0.05 M to 0.30 M at pH 10.0 had a much larger effect as shown in Fig. 7B. Here the initial dissolution rates increase sharply between 0.05 M and 0.15 M Na<sup>+</sup> with a smaller increment between 0.15 M and 0.30 M Na<sup>+</sup>. All of our

subsequent studies were carried out in an added electrolyte concentration of 0.15 M Na<sup>+</sup>.

#### Influence of bile salt concentration on dissolution rates of ChM—static disk method

The initial dissolution rates of ChM (0.15 M Na<sup>+</sup>, 37°C) in CDC and UDC solutions are plotted for four different bile salt concentrations (25–150 mM) in Fig. 8A and 8B respectively. Both CDC and UDC dissolution rates increase strongly with increases in the bile salt concentration and the dissolution rates correlate directly with constant increments in the bile salt concentrations. Over this bile salt concentration range, the equilibrium solubilities of ChM (measured by dissolution to equilibrium) increased linearly from 58 mg/dl in 25 mM to 363 mg/dl in 150 mM CDC solutions and 3.3 mg/dl to 19.0 mg/dl in 25 and 150 mM UDC solutions, respectively. Surprisingly, the cor-

TABLE 1. Static disk experiments: cholesterol solubilities, dissolution rates and dissolution rate constants<sup>a</sup>

	CDC <sup>b</sup>	GCDC	TCDC	UDC	GUDC	TUDC
<b>Cholesterol monohydrate (ChM)</b>						
Equilibrium solubility <sup>c</sup> (mM)	6.1	2.2	1.5	0.33	0.19	0.13
(mg/dl)	(236)	(86)	(57)	(12.8)	(7.5)	(5.0)
Moles of bile salt/mole of cholesterol <sup>d</sup>	16:1	45:1	68:1	303:1	526:1	770:1
Dissolution rate (mmoles·cm <sup>-2</sup> ·sec <sup>-1</sup> ) × 10 <sup>7</sup>	11.2	2.5	1.8	0.39	0.09	0.07
Dissolution rate constant <sup>e</sup> (cm·sec <sup>-1</sup> ) × 10 <sup>4</sup>	2.03	1.25	1.29	1.27	0.46	0.58
<b>Anhydrous cholesterol (ChA)</b>						
Equilibrium solubility <sup>c</sup> (mM)	8.0	3.0	2.0	0.38	0.36	0.28
(mg/dl)	(312)	(116)	(76)	(14.7)	(13.9)	(10.8)
Moles of bile salt/mole of cholesterol <sup>d</sup>	13:1	33:1	50:1	265:1	278:1	357:1
Dissolution rate (mmoles·cm <sup>-2</sup> ·sec <sup>-1</sup> ) × 10 <sup>7</sup>	29.2	5.0	3.6	0.93	n.d. <sup>f</sup>	n.d.
Dissolution rate constant <sup>e</sup> (cm·sec <sup>-1</sup> ) × 10 <sup>4</sup>	4.52	1.86	2.00	2.80	n.d.	n.d.

<sup>a</sup> Conditions were: bile salt concentrations, 100 mM; 0.15 M Na<sup>+</sup>; 37°C, pH 10.0 (free and glycine conjugates) pH 7.0 (taurine conjugates), 25 ml total volume.

<sup>b</sup> See list of abbreviations in text.

<sup>c</sup> Cs in Noyes-Nernst equation (Eq. 1a and 1b).

<sup>d</sup> Saturation ratio, (mol wt of ChA = 387; mol wt of ChM = 403).

<sup>e</sup> "k" in Noyes-Nernst equation (Eq. 1b).

<sup>f</sup> n.d.: not determined.

responding dissolution rate constants (k) were found to be invariant with all bile salt concentrations. The values found were  $2.1 \times 10^{-4}$  (cm·sec<sup>-1</sup>) for 25–150 mM concentrations of CDC and  $1.2 \times 10^{-4}$  (cm·sec<sup>-1</sup>) for the same concentrations of UDC.

#### Influence of increases in temperature on dissolution rates of ChM and ChA in CDC solutions—static disk method

The dissolution rates of ChM and ChA together with their dissolution rate constants (k) and equilibrium cholesterol solubilities (Cs) in 100 mM CDC are summarized in **Table 2**. It is apparent the increases in temperature have only a small effect on equilibrium ChM solubility (Cs). However, since the initial dissolution rates increase dramatically between 17 and 47°C, the rate constants are increased significantly (Table 2). In order to calculate the activation energies of dissolution, the rate constants are plotted according to the Arrhenius equation (**Fig. 9**)

$$E^* = RT^2 \frac{d(\ln k)}{dT} \quad \text{Eq. 5}$$

where E\* is the activation energy in cal/mol, R and T are the gas constant and absolute temperature, respectively, and k is the dissolution rate constant. The graph (**Fig. 9**) indicates that the functional dependence of k on 1/T is linear for both ChM and ChA with slightly different slopes. These slopes give activation energies of 13.7 kcal/mol for ChM dissolution and

10.4 kcal/mol for ChA dissolution. In view of their magnitude, the values strongly suggest that cholesterol dissolution in bile salt solutions is non-diffusion-controlled since E\* for a diffusion-controlled process should be less than 6 kcal/mol (18). The curves when extrapolated to higher temperatures intersect at 86.7°C. This temperature is identical to the first thermotropic phase transition temperature ( $86.4 \pm 0.5^\circ\text{C}$ ) of ChM in excess water observed by differential scanning calorimetry (8) and which has been shown by X-ray diffraction to represent the conversion of ChM to ChA (8).

#### Dissolution of ChM and ChA in CDC solutions—rotating disk method and the Levich equation (Eq. 2)

In order to examine critically whether ChM and ChA dissolution in bile salt solutions is "diffusion-controlled" or "non-diffusion-controlled," we carried out dissolution studies at different r.p.m. (40–800) employing rotating disks of ChM and ChA in 50 ml of 100 mM CDC (pH 10.0, 37°C) as described in Methods. The initial dissolution rates of cholesterol are plotted in **Figs. 10A** and **10B** and show increases in rates as a function of r.p.m. with ChA being uniformly faster than ChM. These values together with the angular velocities ( $\omega$ ), Reynolds numbers, and dissolution rate constants are summarized in **Table 3**. By plotting the k values (Table 3) for both ChA and ChM dissolution according to Eq. 2 (of Levich), it is apparent (**Fig. 11A**) that the data fall on two linear



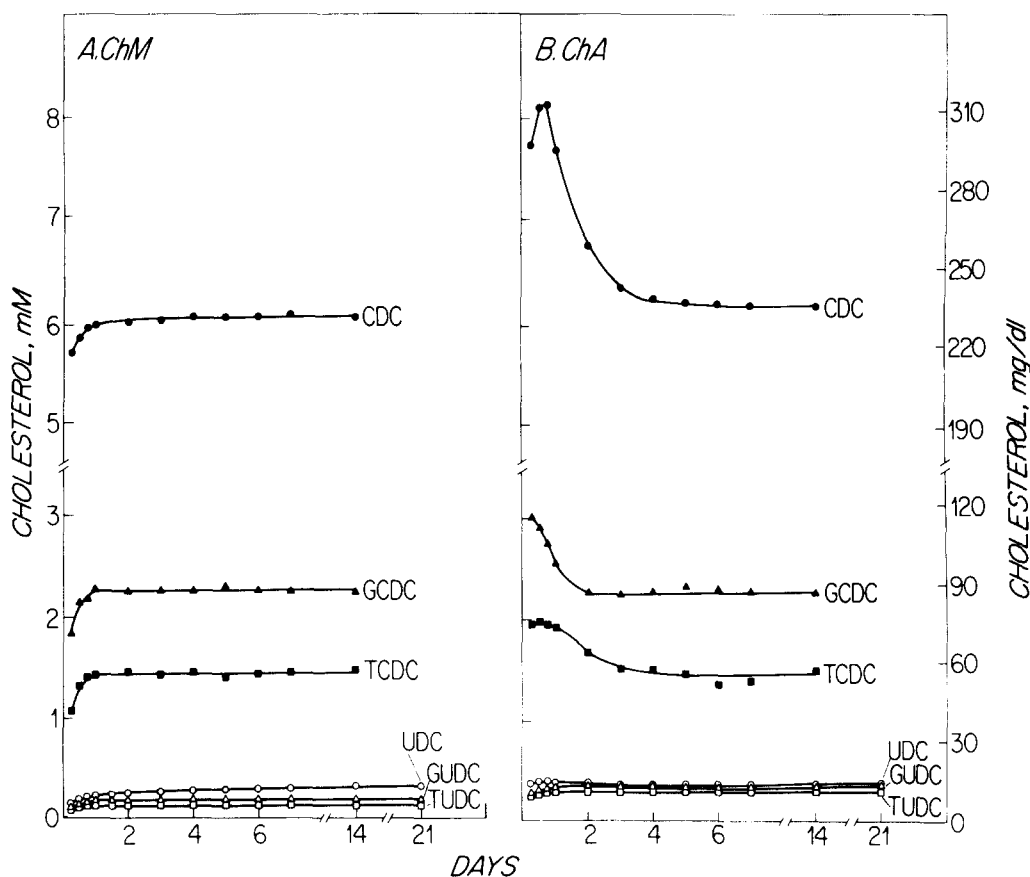


Fig. 6. Dissolution rates of powder slurries of A: cholesterol monohydrate (ChM) and B: anhydrous cholesterol (ChA) in 100 mM bile salt solutions (continuous shaking, 37°C, 0.15 M Na<sup>+</sup>, pH 7.0 (taurine conjugates) and pH 10.0 (free and glycine conjugates)). See list for bile salt abbreviations.

regressions which, when extrapolated to the ordinate, give positive intercepts (ChM > ChA). If dissolution of cholesterol by bile salts were diffusion-controlled, these extrapolations should pass through the origin as was observed with benzoic acid (Fig. 3).

In order to validate this conclusion unequivocally, the results of Fig. 11A are replotted in Fig. 11B, according to Eq. 4a. The positive intercepts now give the reciprocals of the interfacial rate constants ( $k_r$ ) and the fact that the curves are parallel in the mid-range of rotating speeds (80–300 r.p.m.) suggests that the product of the diffusion coefficients ( $D$ ) and the kinematic viscosity ( $\nu$ ) are constant over this range. This plot confirms that the interfacial reaction rate of ChA is faster than ChM and, since the intercept is not zero, confirms that dissolution is non-diffusion-controlled.

#### Simulation of physiological flow conditions—stagnant dissolution of ChM in bile salt solutions

Since bile bathing a cholesterol gallstone within the gallbladder is for all intents an unstirred system, stagnant (no-stirring) dissolution experiments were

conducted employing static disks of ChM as described in Methods. The results for dissolution studies in which UDC and GUDC were compared with CDC

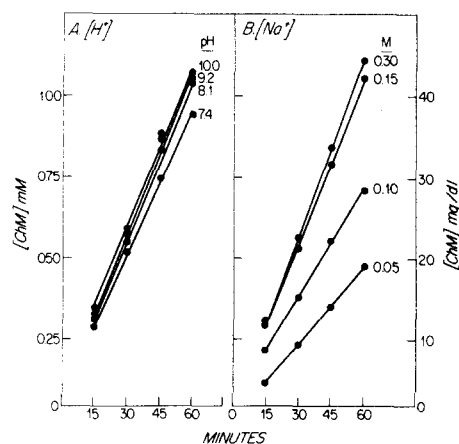
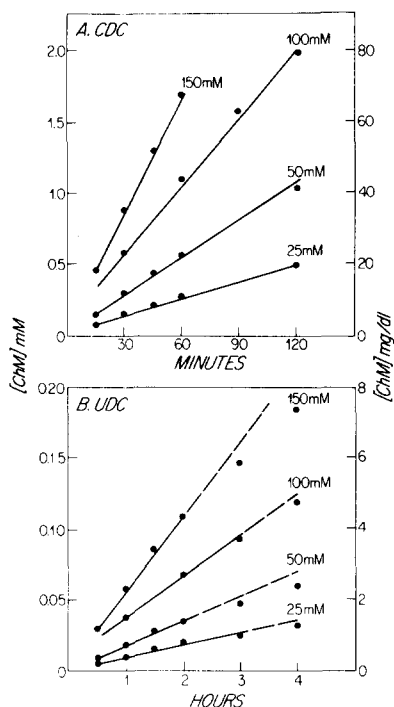
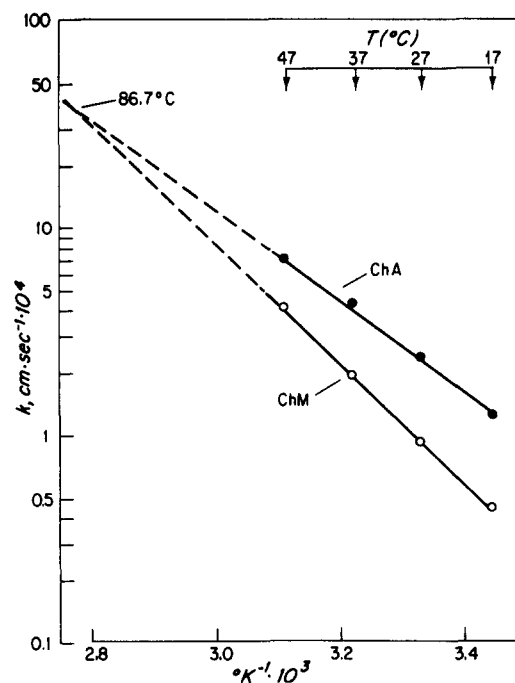


Fig. 7. Influence of A: bulk pH and B: ionic strength (Na<sup>+</sup>) on the initial dissolution rates of cholesterol monohydrate (ChM) in 100 mM CDC solutions (37°C, 300 r.p.m., static disk method). In A, the ionic strength is 0.15 M Na<sup>+</sup>; in B, ionic strength varies from 0.04–0.29 M NaCl plus 0.01 M carbonate–bicarbonate buffer (pH 10.0).



**Fig. 8.** Influence of different bile salt concentration (25–150 mM) on the initial dissolution rates of cholesterol monohydrate (ChM) in A, CDC and B, UDC solutions. (37°C, 300 r.p.m., pH 10.0, 0.15 M Na<sup>+</sup>, static disk method). Note differences between A and B with respect to the scales of both ordinate and abscissa.

and GCDC are summarized in **Table 4**. Under these conditions the dissolution rates are much reduced for both bile salt species compared with the stirred conditions, but in all cases the initial dissolution rates and rate constants for UDC and GUDC are still appreciably smaller than those for CDC and GCDC.



**Fig. 9** Arrhenius plots of dissolution rate constants ( $k$ ) for ChA and ChM in 100 mM CDC solutions (pH 10.0, 0.15 M Na<sup>+</sup>, 300 r.p.m., 17–47°C; static disk method) plotted as a function of inverse degrees Kelvin (°K). The temperature corresponding to the extrapolated intersection of the curves (86.7°C) corresponds to the transition temperature of ChM → ChA. The slopes give the activation energies of dissolution in cal/mole (see text).

## DISCUSSION

Our aim in this study was to compare the dissolution kinetics of artificial cholesterol gallstones (“cholesterol disks”) in micellar solutions of CDC and its conjugates with UDC and its conjugates. Since both bile

**TABLE 2.** Influence of temperature on cholesterol dissolution rates and micellar solubilities<sup>a</sup>

Temperature	Cholesterol Monohydrate				Anhydrous Cholesterol			
	17°C (290°K)	27°C (300°K)	37°C (310°K)	47°C (320°K)	17°C (290°K)	27°C (300°K)	37°C (310°K)	47°C (320°K)
	( <i>ChM</i> ) mg/dl				( <i>ChA</i> ) mg/dl			
Time (minutes)								
15	2.5	5.4		25.4	9.6	17.9		52.7
30	5.0	10.7	23.4	48.3	18.9	34.8	56.3	96.8
45	7.5	15.9		68.8	27.9	50.6		133.9
60	9.9	21.0	43.8	87.3	36.6	65.5	115.0	165.0
{60} <sup>b</sup>	9.94	21.1		89.6	36.9	66.5		171.9
Dissolution rate constant <sup>c</sup> (cm·sec <sup>-1</sup> × 10 <sup>4</sup> )	0.47	0.98	2.03	4.34	1.33	2.46	4.52	7.30
Equilibrium cholesterol solubility <sup>d</sup> (mg/dl)	212	223	236	251	291	300	312	327

<sup>a</sup> Static disk method; (100 mM chenodeoxycholate, 0.15 M Na<sup>+</sup>, pH 10.0, volume of micellar solution, 25 ml).

<sup>b</sup> Values from a least squares linear regression of initial dissolution rate data.

<sup>c</sup> “ $k$ ” value in Eq. 1b.

<sup>d</sup> “ $C_s$ ” value in Eq. 1b.

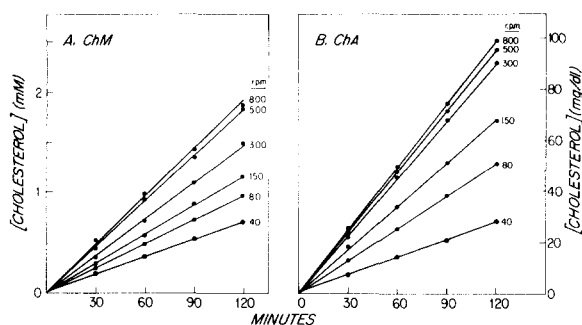


**Fig. 10.** Influence of rotating disk speed (r.p.m.) on the initial dissolution rates of A, cholesterol monohydrate (ChM) and B, anhydrous cholesterol (ChA) in 100 mM CDC (37°C, pH 10.0, 0.15 M Na<sup>+</sup>, 50 ml solutions).

acids are now commonly employed for the medical dissolution of gallstones, we hoped to identify why UDC, a poor detergent in terms of in vitro cholesterol solubilizing capacity (7) and confirmed here (Fig. 6A), could be capable of producing clinical results apparently comparable in efficiency to CDC (6), which is a good solubilizer of cholesterol (Fig. 6A). Since gallstone dissolution clinically is an extremely slow process, we were also interested in identifying physical-chemical conditions which might be therapeutically useful in accelerating dissolution. Last, we felt that it was important to compare and contrast the dissolution of the two major crystalline forms of cholesterol, ChA and ChM, for the reasons indicated in the introduction and because one group of investigators (21) did not characterize the physical state of cholesterol in their dissolution studies (but probably employed ChA since no precautions were taken to prepare the monohydrate). For this reason, the question as to whether cholesterol gallstone dissolution is diffusion-controlled or not is still a matter of

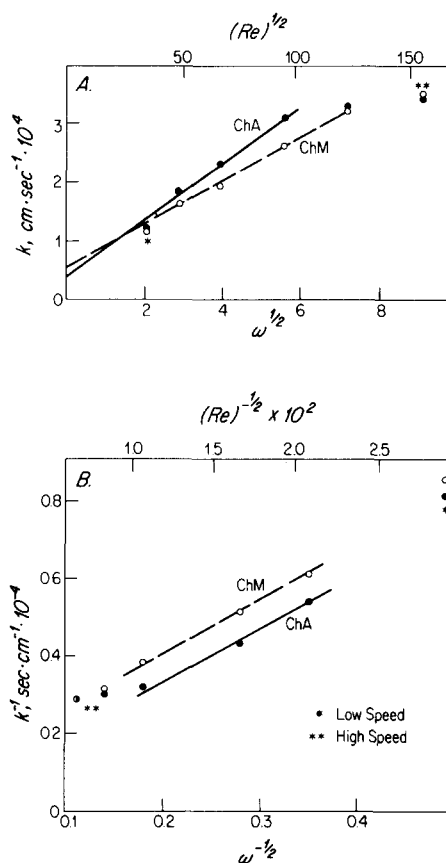


**Fig. 11.** Levich equation (Eq. 2) plots of dissolution rate constants ( $k$ ) of ChA and ChM in 100 mM CDC solutions (pH 10.0, 37°C, 0.15 M Na<sup>+</sup>, rotating disk method) as a function of the square root of the rotating speed ( $\omega^{1/2}$ ) and Reynold's number ( $Re^{1/2}$ ). In A,  $k$  is plotted against  $\omega^{1/2}$  according to Eq. 2. In B,  $k^{-1}$  is plotted against  $\omega^{-1/2}$  according to Eq. 4a (see text for details).

dispute. Our study confirms and extends the pioneering and detailed studies of Higuchi and his school (11, 23, 24–26) on the dissolution kinetics of choles-

TABLE 3. Rotating disk experiments: influence of rotation speed on dissolution rates and dissolution rate constants<sup>a</sup>

R.P.M. <sup>d</sup>	$\omega^e$	$\omega^{1/2}$	$(Re^{1/2})^f$	Cholesterol Monohydrate (ChM) <sup>b</sup>				$k^c$	Anhydrous Cholesterol (ChA) <sup>b</sup>				$k^c$
				Time (min)					Time (min)				
40	4.02	2.05	(34.73)	7.1	13.9	20.7	27.1	1.18	7.3	14.4	21.3	28.0	1.22
80	8.38	2.89	(49.13)	10.4	19.0	27.3	38.1	1.64	13.0	25.7	38.7	37.0	1.84
150	15.71	3.96	(67.26)	10.9	21.4	33.5	45.7	1.96	18.1	34.3	57.3	68.0	2.30
300	31.42	5.60	(95.13)	13.3	28.2	43.4	62.5	2.62	22.8	45.9	68.0	90.4	3.10
500	52.36	7.24	(122.80)	17.1	36.5	52.8	73.4	3.24	23.9	48.1	71.6	96.1	3.28
800	83.78	9.15	(155.33)	20.6	38.8	56.6	74.1	3.46	25.7	49.9	74.5	99.4	3.42

<sup>a</sup> 100 mM chenodeoxycholate, pH 10.0, 0.15 M Na<sup>+</sup>, 37°C, 50 ml solutions.

<sup>b</sup> Micellar cholesterol solubilities expressed in mg/dl.

<sup>c</sup> cm·sec<sup>-1</sup> × 10<sup>4</sup>.

<sup>d</sup> Rotating speed of cholesterol disk in revolutions per minute.

<sup>e</sup> Angular velocity in radians sec<sup>-1</sup> ( $\omega = 2\pi \times \text{R.P.S.}$ ).

<sup>f</sup> Square root of Reynold's number for this experimental system (see footnote 4).

TABLE 4. Static disk method: stagnant (unstirred) dissolution of cholesterol monohydrate<sup>a</sup>

Bile Salt	Cholesterol Solubilized (mg/dl)					$y = b$	Initial Dissolution Rate (mmol·cm <sup>-2</sup> ·sec <sup>-1</sup> × 10 <sup>7</sup> )	Dissolution Rate Constant (k) (cm·sec <sup>-1</sup> × 10 <sup>4</sup> )
	Time (Hr)							
	1	2	4	6	8			
UDC <sup>c</sup>	(0.42) <sup>d</sup>	0.85	1.57	2.29	2.98	0.37x + 0.048	0.11	0.32
CDC	(11.9)	23.8	46.0	68.3	90.5	11.28x + 0.62	3.0	0.50
GUDC	(0.21)	0.38	0.83	1.15	1.45	0.18x + 0.028	0.07	0.28
GCDC	(2.7)	5.29	12.39	18.66	25.69	3.24x + 0.54	0.69	0.31

<sup>a</sup> 100 mM bile salt solutions; ChM disks; 0.15 M Na<sup>+</sup>; pH 10.0; 37°C. 25 ml solutions.

<sup>b</sup> Linear regression equations for 0–8 hr of stagnant dissolution.

<sup>c</sup> See abbreviation list in text.

<sup>d</sup> Represents interpolated values employing the linear regression equations in <sup>b</sup>.

terol monohydrate with bile salts. In particular, our studies extend this work to UDC and its conjugates and confirm, under all conditions, that ChA and ChM gallstone dissolution is non-diffusion-controlled, results which directly contradict the conclusion of Tao, Cussler, and Evans (21) who concluded that convection/diffusion rather than the interfacial reaction was the major determinant of the dissolution rate.

We found that three different experimental methods were required in these studies. The static disk method provides dissolution rates (mmol·cm<sup>-2</sup>·sec<sup>-1</sup>), the dissolution rate constant (cm·sec<sup>-1</sup>), and the equilibrium solubility of cholesterol (mM). The rotating disk method with the use of the Levich equation (Eq. 2) distinguishes whether dissolution of cholesterol by bile salts is diffusion-controlled or not, i.e., possessing an interfacial component. This is illustrated in Fig. 12 which shows the postulated mechanisms of cholesterol dissolution as three conductances in series: two diffusional steps and one interfacial step. The powder dissolution method together with disk dissolution gives good estimates of the apparent equilibrium micellar solubility of ChA but in addition allows, under favorable circumstances, the hydration and nucleation of supersaturated systems derived from ChA (Fig. 6B). Finally, limited experiments were carried out with ChM disks in stagnant (unstirred) bile salt solutions and show that many of the trends developed in this work can be extrapolated to unstirred gallbladder bile.

### Influences of cholesterol monohydrate and anhydrous cholesterol

ChM differs from ChA in the nature of the molecular packing within the triclinic crystals and hence in their X-ray powder diffraction patterns and crystal habits as shown in Fig. 13 (adapted from Ref. 8, 27, 28). That differences in ChA and ChM solubility and dissolution rates might occur in bile salt solutions was originally emphasized by Mufson et al. (29, 30), who

examined cholesterol solubility in conjugated bile salt-lecithin systems, and by Shefter and Higuchi (31), who studied the dissolution rates of ChA and ChM in 50% glycerol-ethanol systems. These investigators demonstrated that the initial dissolution rate of ChA was 3 times faster than ChM and that ChA solubility was 1.4 times as great as the solubility of the monohydrate. Further, the dissimilar dissolution rates of many drugs are the result of the fact that they exist in anhydrous and hydrated crystalline forms (31). The preparation of anhydrous forms has been suggested as a practical measure to enhance their solubilization and absorption from the gastrointestinal tract (32).

In the static disk experiments, ChA solubility in each bile salt micellar system (Fig. 5) reached a plateau and leveled off at values appreciably greater than those found with ChM. These values for ChA most likely reflect equilibrium micellar solubilities since, over the time course of these experiments, nucleation did not occur. In contrast, when ChA powder slurries were studied (Fig. 6), solubilities peaked at levels identical to those of the plateau region for ChA disks (Fig. 5B) during the first day of dissolution. There-

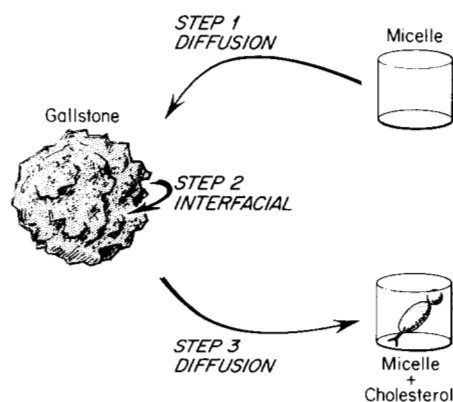
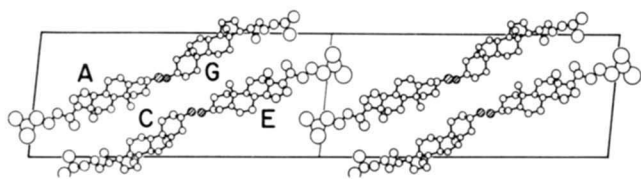


Fig. 12. Highly schematicized diagram of the three theoretical steps in the overall process of cholesterol gallstone dissolution.

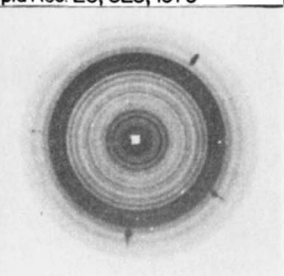
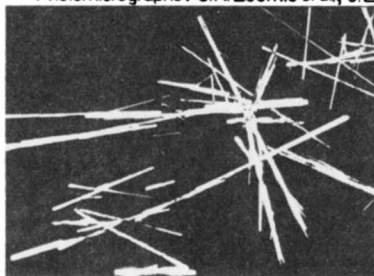
## ANHYDROUS CHOLESTEROL



H.S. Shieh *et al.*, *Nature* 267, 287, 1977

B.M. Craven, *Nature* 260, 727, 1976

Photomicrographs: C.R. Loomis *et al.*, *J. Lipid Res.* 20, 525, 1979



## CHOLESTEROL MONOHYDRATE

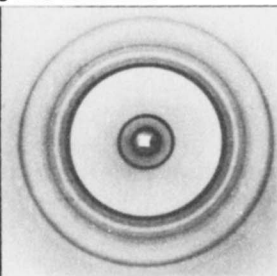
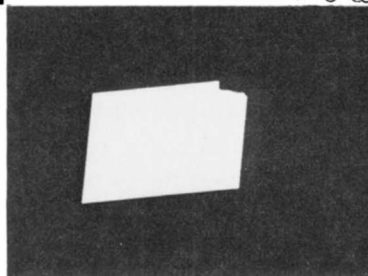
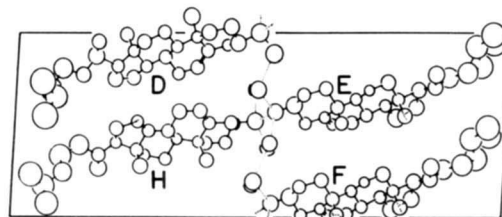
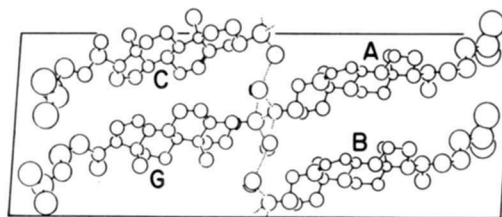
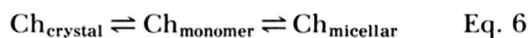


**Fig. 13.** Crystal habits, high- and low-angle X-ray powder diffraction patterns and unit cell crystallographic structures of anhydrous cholesterol (ChA) and cholesterol monohydrate (ChM). Reproduced from refs. 8, 27, and 28 with kind permission of the copyright owners (MacMillan Publications and Lipid Research Inc.) and the authors.

after, the solubilities of 'ChA' decreased to level off at values equivalent to equilibrium ChM solubilities and hence reflected a change in micellar solubility of cholesterol due to the conversion of ChA to ChM. Thus the attempt of the system to achieve equilibrium solubility of ChA (as in the disk experiments) is rapidly counteracted by a change in micelle solubility due to hydration of ChA  $\rightarrow$  ChM and continuous nucleation in the presence of excess cholesterol. In the present studies, not only were equilibrium micellar solubilities of ChA (Table 1, Fig. 5) 1.2 to 2.2 (mean 1.53)-times greater than the micellar solubility of ChM, but dissolution rates were 2 to 3-fold faster. Based on our previous analysis of the molecular determinants of ChM solubility in bile salt micelles (33), we can conclude that the monomeric aqueous solubility of ChA must be greater than ChM and hence would be a factor in accelerating the dissolution rates. However, the crystal lattice energy may also be important in the dissolution process since the micellar binding of cholesterol is the result of two coupled equilibria



As shown in Fig. 13, the ChM bilayer in the unit

cell is held together by strong H-bonding to an inter-linked lattice of H<sub>2</sub>O molecules, whereas in the unit cell of ChA only weak H-bonds between opposing OH groups of two cholesterol molecules are involved (27, 28). The prolonged (21-day) metastability of solubilized ChA in the UDC conjugates (Fig. 6) is most likely to be related to resistance to nucleation rather than hydration, since our results for CDC (Fig. 6) show that powdered ChA is hydrated in 2–6 days. This finding is paralleled by the extensive metastable solubility of the insoluble protonated form of UDC and GUDC when solubilized by their own micelles during potentiometric titration (9). As emphasized by Mufson *et al.* (30) and Carey and Small (10) earlier, the micellar solubility of cholesterol when dried from organic solvents (method of coprecipitation) is quite similar to the present ChA solubility results (Fig. 6B) since the cholesterol initially formed by this process is anhydrous. Hence, if sufficient time is not allowed for equilibration (hydration of ChA and nucleation and precipitation of excess ChM), falsely high values of "ChM" solubility will be obtained. For reasons outlined above, it is apparent that true equilibrium solubilities of ChM in UDC micelles can only

be derived from equilibrium dissolution experiments (see Fig. 6A and 6B).

### Influence of bile salt type

Dissolution with CDC and its conjugates was markedly faster than with UDC and its conjugates under all circumstances. These results can in part be explained by the greater capacity of the CDC series to solubilize cholesterol. In fact as shown in Fig. 14, when all of the common bile salts are compared, the initial dissolution rates correlate directly with equilibrium cholesterol solubility irrespective of the bile salt species and crystalline form of cholesterol.<sup>6</sup> It is of interest that the rank-ordering of dissolution rates is CDC series > DC series > C series > UDC series and in all cases free bile salts are faster than G-conjugates which in turn are faster than T-conjugates. Since the dissolution rates of each bile salt series fall on separate curves, it is obvious that other physical-chemical properties of the bile salts significantly influence their cholesterol dissolution rates. It is unlikely that the variations in micellar size and diffusion coefficients of the micelles (34) are responsible for these results since the present studies were carried out at 300 r.p.m. where micellar diffusion would play only a minor role in controlling the overall dissolution rate. Therefore, we suggest that different interfacial reaction rates are the predominant factors responsible for variations in the dissolution rates shown in Fig. 14. In the case of the cholelitholytic species, when the data for UDC/GUDC/TUDC and CDC/GCDC/TCDC are plotted semilogarithmically, they fall on two separate linear regressions (not shown). The dissolution rate for the UDC series is  $1.32 \text{ mmoles} \cdot \text{cm}^{-2} \cdot \text{sec}^{-1}$  per 1 mM increment in cholesterol solubility versus  $2.1 \text{ mmoles} \cdot \text{cm}^{-2} \cdot \text{sec}^{-1}$  per 1 mM increment in solubility for the CDC series. This suggests that the interfacial reaction rate may well be slower in the case of dissolution with the UDC series. Direct rotating disk experiments will be necessary to confirm this possibility.

### Important effects of pH, bile salt, and electrolyte concentrations

Provided the bile salt is fully ionized, a change in pH (Fig. 7A) has essentially no effect on dissolution rate. When micelles become progressively saturated with the protonated species to form mixed bile salt-bile acid micelles (9), such as occurs in the case of CDC at pH 7.4, dissolution is retarded. This implies

<sup>6</sup> This relationship is predicted by Equation 3b where the initial dissolution rate  $(dC/dt)_{t \rightarrow 0}$  is proportional to the equilibrium cholesterol solubility ( $C_s$ ).

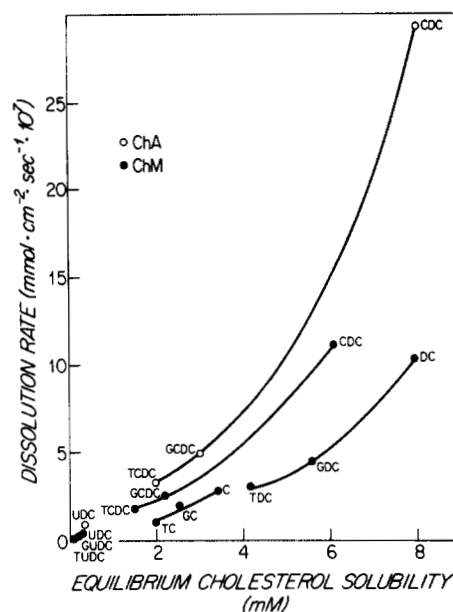


**Fig. 14.** Relationship between the initial dissolution rates of both ChA and ChM by the common bile salt species of man, C, DC, CDC, UDC, and their T and G conjugates and equilibrium cholesterol solubilities in 100 mM bile salt solutions (0.15 M Na<sup>+</sup>, 37°C). ChM solubilities in the C and DC series were measured by dissolution to equilibrium (M. J. Armstrong and M. C. Carey. Unpublished observations).

that micellized bile acids and cholesterol compete for binding sites within micelles. Since GUDC has a high precipitation pH (9) and predominates in bile of patients on UDC therapy, this suggests that a slightly acid gallbladder bile might be inimical to the success of dissolution. We have previously discussed (9) how taurine feeding should offset this disadvantage, a suggestion further reinforced by our data in Fig. 7A.

As was previously shown by Kwan et al. (25) and confirmed here, increases in both bile salt and neutral electrolyte concentrations promote dramatic increases in dissolution rates (Fig. 7B, Fig. 8A and B). In the former case, dissolution is enhanced by the increase in the capacity of the system to solubilize cholesterol. In fact, the slopes of the data in Fig. 8 clearly indicate that the increment in dissolution rates is directly proportional to the bile salt concentration.

With reference to the effects of ionic strength, it is now generally accepted (10, 25) that increases in neutral electrolyte concentration, by progressively shielding the net negative charge on the micelles, promotes access of micelles from the bulk to the solid-solution interface. Hence more micelles can detach cholesterol molecules simultaneously. The smaller dissolution increment between 0.15 M and 0.3 M Na<sup>+</sup> in the case of CDC (Fig. 7B) strongly suggests that charge shielding may be counterbalanced by the formation of large secondary micelles (34). A similar

hypothesis has recently been advanced for the promotion of dissolution by cationic detergents and alkyl amines which bind tightly to and hence shield the charges of bile salt micelles (35).

### The role of the interface—non-diffusion control

That the interfacial reaction at the cholesterol-dissolution interface plays a key role in the overall process of gallstone dissolution was first proposed by Higuchi and associates (36). In this scheme (Fig. 12), the rate of detachment of cholesterol molecules from the interface is slow compared with the diffusion steps. Tao et al. (21) have claimed that gallstone dissolution is diffusion-controlled even under stagnant conditions but since ChA was probably employed, this together with experimental errors could account for their results being closer to the diffusion-controlled limit (see Fig. 11A). The results of our experiments (Fig. 11A and B) are in general agreement with Higuchi's results (23, 25). First, a plot of  $k$  values against  $\omega^{1/2}$  in the midrange of rotating speeds for both ChA and ChM clearly shows that Levich's equation (Eq. 2) is not obeyed since the extrapolated curve gives a positive intercept. Prakongpan et al. (23) actually carried out rotating disk experiments with ChM and sodium cholate at very low rotating speeds ( $\sqrt{Re} = 33$ ) and showed, as in the present work, that the interfacial reaction plays the dominant role as the rate-determining step in cholesterol dissolution. The numerical values for dissolution rates obtained by Patel and Higuchi (35) and Higuchi et al. (36), when normalized for our conditions of stirring speeds and disk compression, give results that are quite comparable to our values for all the common bile salts in Fig. 14.

Further support for the importance of the interfacial reaction in controlling both ChA and ChM dissolution can be inferred from the large activation energies (10.4 and 13.7 kcal/mol, respectively) obtained from the Arrhenius plots in Fig. 9 (18). The convergence of the slopes of the ChA and ChM curves as the temperature is increased is likely to be related to the concentration of ChA and ChM monomers in equilibrium with the solid crystals and with the molecules bound to micelles (Eq. 10). As the temperature is increased, the monomer equilibria become more biased toward ChA since more ChA monomers will be present in solution. Hence, the intersection of these curves (86.7°C) accurately corresponds to the sharp cholesterol hydrate  $\rightarrow$  anhydrate transition temperature (86.4°C) found by Loomis et al. (8). The linearity of the curve for ChA at temperatures above and below its polymorphic crystalline transition temperature (39°C) (8) suggests that the dissolution rates of the low-temperature anhydrous crystal

polymorphs are not influenced by an alteration in the crystal packing.


### Physical interpretation of the interfacial reaction

When dissolution of a substance is diffusion-controlled, a thin layer of solvent in contact with the solid interface becomes completely saturated (Fig. 2). Hence if molecules cannot move out of the saturated layer, dissolution becomes terminated such as in an idea stagnant situation. As shown in Fig. 3 for benzoic acid (one of the few substances whose dissolution is nearly diffusion-controlled) in the total absence of stirring ( $\sqrt{Re} = 0$ ) no instantaneous dissolution should be possible (see footnote<sup>5</sup>). In the non-diffusion controlled situation (Fig. 2B), the layer of solvent next to the solid always shows a concentration gradient ( $C_s - C_i$ ) because the surface detachment of molecules is extremely slow, hence molecules will flow into the bulk solution across the diffusion layer owing to the presence of a diffusion gradient. It is of interest in this regard that the positive intercept for ChM in Fig. 11A gives a dissolution rate constant ( $k$ ) of  $0.54 \times 10^{-4} \text{ cm} \cdot \text{sec}^{-1}$ . This value is essentially identical to the  $k$  value of  $0.5 \times 10^{-4} \text{ cm} \cdot \text{sec}^{-1}$  derived entirely by experiment for ChM dissolution in the stagnant study (Table 4).

### Conclusions and physiological implications

We have established in these studies *i*) that the dissolution kinetics of ChA and ChM by bile salts is non-diffusion-controlled; *ii*) that CDC and its conjugates are much more effective solubilizers of ChM and ChA in terms of capacity (an equilibrium event) and rate (a kinetic event) than UDC and its conjugates and that within each species the ordering of solubilities and dissolution rates is free salts > glycine conjugates > taurine conjugates; *iii*) that the solubilities and dissolution rates of ChA by both species are significantly greater than ChM, this higher thermodynamic activity being related to a more rapid interfacial reaction at the surface of the anhydrous crystal, possibly due to a higher monomeric aqueous solubility of the ChA monomers compared to the ChM monomers; and *iv*) that the dissolution rates are accelerated in direct proportion to bile salt and neutral electrolyte concentration and retarded appreciably when the bile salt species becomes partly protonated.

Human bile in a mixed micellar system contains appreciable quantities of lecithin (10). This key variable is known to retard the dissolution rate of ChM by the common bile salts (25) and to narrow the differences in equilibrium solubility between CDC and UDC conjugates (7), hence any prediction of physiological importance for cholesterol gallstone dissolu-

tion must be extremely guarded on the basis of studies with pure bile salt systems. If, as a first approximation, the influence of equivalent lecithin contents in mixed micellar systems applies equally to the CDC and UDC species and if the total lipid concentration and bile salt to lecithin ratios in bile are the same on cheno- and ursotherapy, then we can predict that clinical gallstone dissolution with micelles enriched in UDC conjugates must be slower than with CDC conjugates. Yet it has been claimed, on the basis of a large number of clinical dissolution studies, that UDC is as effective as CDC in vivo (6). To explain this apparent paradox, a novel possibility has been suggested recently (37) and has been confirmed by us,<sup>7</sup> that a liquid-crystalline mesophase may form during cholesterol dissolution with conjugated UDC-lecithin mixtures and may be clinically important in accelerating gallstone dissolution. 

We thank Dr. Marc Grympas (Children's Hospital Medical Center, Boston, MA) for X-ray powder diffraction measurements, and Dr. Marcia J. Armstrong and Dr. Yong Hyun Park (Peter Bent Brigham Hospital Boston, MA) for their help with HPLC and some of the dissolution experiments. Dr. H. Igimi's permanent address is First Department of Surgery, Fukuoka University School of Medicine, Fukuoka, Japan. Dr. M. C. Carey is recipient of a Research Career Development Grant from the National Institutes of Health (AM 00195). The research was supported in part by Research Grant AM 18559 (NIAMDD).

Manuscript received 4 August 1980 and in revised form 30 September 1980.

## REFERENCES

1. Bogren, H., and K. Larsson. 1963. Crystalline components of biliary calculi. *Scand. J. Clin. Lab. Invest.* **15**: 557-558.
2. Miyake, H., and C. G. Johnston. 1968. Gallstones: ethnological studies. *Digestion.* **1**: 219-228.
3. Small, D. M., and G. G. Shipley. 1974. Physical-chemical basis of lipid deposition in atherosclerosis. *Science.* **185**: 222-229.
4. Small, D. M. 1977. Liquid crystals in living and dying systems. *J. Colloid Interface Sci.* **58**: 581-602.
5. Stiehl, A., P. Czygan, B. Kommerell, H. J. Weiss, and K. H. Holtermüller 1978. Ursodeoxycholic acid versus chenodeoxycholic acid. Comparison of their effects on bile acid and bile lipid composition in patients with cholesterol gallstones. *Gastroenterology.* **75**: 1016-1020.
6. Nakayama, F. 1980. Oral cholelitholysis—cheno versus urso. *Dig. Dis. Sci.* **25**: 129-134.

<sup>7</sup> Igimi, H., G. Salvioli, and M. C. Carey. Unpublished observations.

7. Carey, M. C. 1978. Critical tables for calculating the cholesterol saturation of native bile. *J. Lipid Res.* **19**: 945-955.
8. Loomis, C. R., G. G. Shipley, and D. M. Small. 1979. The phase behavior of hydrated cholesterol. *J. Lipid Res.* **20**: 525-535.
9. Igimi, H., and M. C. Carey. 1980. pH-Solubility relations of chenodeoxycholic and ursodeoxycholic acids: physical-chemical basis for dissimilar solution and membrane phenomena. *J. Lipid Res.* **21**: 72-90.
10. Carey, M. C., and D. M. Small. 1978. The physical chemistry of cholesterol solubility in bile: relationship to gallstone formation and dissolution in man. *J. Clin. Invest.* **61**: 998-1026.
11. Higuchi, W. I., S. Prakongpan, and F. Young. 1973. Mechanisms of dissolution of human cholesterol gallstones. *J. Pharm. Sci.* **62**: 945-948.
12. Igimi, H. 1972. Experimental studies on dissolution of cholesterol stones. *Acta Med.* **42**: 55-66.
13. Fromm, H., P. Amin, H. Klein, and I. Kupke. 1980. Use of a simple enzymatic assay for cholesterol analysis in human bile. *J. Lipid Res.* **21**: 259-261.
14. Carr, J. J., and I. J. Dreckter. 1956. Simplified rapid technique for the extraction and determination of serum cholesterol without saponification. *Clin. Chem.* **2**: 353-368.
15. Noyes, A. A., and W. R. Whitney. 1897. The rate of solution of solid substances in their own solutions. *J. Am. Chem. Soc.* **19**: 930-934.
16. Nernst, W. 1904. Theorie der Reaktionsgeschwindigkeit in heterogenen Systemen. *Z. Physikal. Chem.* **47**: 52-55.
17. Levich, V. G. 1962. Physicochemical Hydrodynamics. Prentice-Hall, Inc., Englewood Cliffs, NJ. 60-72.
18. Nogami, H., T. Nagai, E. Fukuoka, and T. Yoksunyanagi. 1969. Dissolution kinetics of barbital polymorphs. *Chem. Pharm. Bull.* **17**: 23-31.
19. Wurster, D. E., and P. W. Taylor. 1965. Dissolution kinetics of certain crystalline forms of prednisolone. *J. Pharm. Sci.* **54**: 670-676.
20. Berthoud, A. 1912. Théorie de la formation des faces d'un cristal. *J. Chem. Phys.* **10**: 624-635.
21. Tao, J. C., E. L. Cussler, and D. F. Evans. 1974. Accelerating gallstone dissolution. *Proc. Nat. Acad. Sci. USA* **71**: 3917-3921.
22. Gibaldi, M., S. Feldman, R. Wyan, and N. D. Werner. 1968. Dissolution rates in surfactant solutions under stirred and static conditions. *J. Pharm. Sci.* **57**: 787-791.
23. Prakongpan, S., W. I. Higuchi, K. H. Kwan, and A. M. Molokhia. 1976. Dissolution rate studies of cholesterol monohydrate in bile acid-lecithin solutions using the rotating disk method. *J. Pharm. Sci.* **65**: 685-689.
24. Higuchi, W. I., F. Squib, D. Mufson, A. P. Simonelli, and A. F. Hofmann. 1973. Dissolution kinetics of gallstones: physical model approach. *J. Pharm. Sci.* **62**: 942-945.
25. Kwan, K. H., W. I. Higuchi, A. M. Molokhia, and A. F. Hofmann. 1977. Dissolution kinetics of cholesterol in simulated bile. I. Influence of bile acid type and concentration, bile acid-lecithin ratio and added electrolyte. *J. Pharm. Sci.* **66**: 1094-1101.
26. Kwan, K. H., W. I. Higuchi, and A. F. Hofmann. 1978. Dissolution kinetics of cholesterol in simulated bile. II. Influence of simulated bile composition. *J. Pharm. Sci.* **67**: 1711-1714.



27. Craven, B. M. 1976. Crystal structure of cholesterol monohydrate. *Nature*. **260**: 727–729.
28. Shieh, H. S., L. G. Hoard, and C. E. Nordman. 1977. Crystal structure of anhydrous cholesterol. *Nature* **267**: 287–289.
29. Mufson, D., K. Meksuwan, Z. E. Zarembo, and L. J. Ravin. 1972. Cholesterol solubility in lecithin–bile salt systems. *Science*. **177**: 701–702.
30. Mufson, D., K. Triyanond, Z. E. Zarembo, and L. J. Ravin. 1974. Cholesterol solubility in model bile systems: implications in cholelithiasis. *J. Pharm. Sci.* **63**: 327–332.
31. Shefter, E., and T. Higuchi. 1963. Dissolution behavior of crystalline solvated and non-solvated forms of some pharmaceuticals. *J. Pharm. Sci.* **52**: 781–791.
32. Higuchi, T. 1958. Some physical chemical aspects of suspension formulation. *J. Am. Pharm. Assoc. Sci. Ed.* **47**: 657–660.
33. Mazer, N. A., G. B. Benedek, and M. C. Carey. 1978. What determines the limits of cholesterol solubility in model bile systems? *Gastroenterology*. **75**: 976 (Abstract).
34. Mazer, N. A., M. C. Carey, R. Kwasnick, and G. B. Benedek. 1979. Quasielastic light-scattering studies of aqueous biliar lipid systems. Size, shape and thermodynamics of bile salt micelles. *Biochemistry*. **18**: 3064–3075.
35. Patel, D. C., and W. I. Higuchi. 1980. Mechanism of cholesterol gallstone dissolution. II. Correlation between the effect of alkyl amines as cholesterol gallstone dissolution rate accelerators and the degree of binding of the alkyl amines to bile acid micelles. *J. Colloid Interface Sci.* **74**: 211–219.
36. Higuchi, W. I., S. Prakongpan, V. Surpurinya, and F. Young. 1972. Cholesterol dissolution rate in micellar bile acid solutions: retarding effect of added lecithin. *Science*. **178**: 633–634.
37. Corrigan, O. I., C. C. Su, W. I. Higuchi, and A. F. Hofmann. 1980. Mesophase formation during cholesterol dissolution in ursodeoxycholate–lecithin solution: new mechanism for gallstone dissolution in humans. *J. Pharm. Sci.* **69**: 869–870.